Study of the aerodynamics of a full-scale tractor-trailer

Junshuai Wang[1], Xinfeng Zhang[2], Linglong Wang[3], Fengyang Liu[4], Zhenguo Liu[5]
CATARC Component Technology (Tianjin) Co., Ltd, Tianjing, 300300, China
[1]Corresponding author
E-mail: [1]*wangjunshuai@catarc.ac.cn*, [2]*zhangxinfeng@catarc.ac.cn*, [3]*wanglinglong@catarc.ac.cn*, [4]*liufengyang@catarc.ac.cn*, [5]*liuzhenguo@catarc.ac.cn*

Received 8 January 2025; accepted 9 February 2025; published online 15 May 2025
DOI https://doi.org/10.21595/vp.2025.24771

Check for updates

72nd International Conference on Vibroengineering in Almaty, Kazakhstan, May 15-16, 2025

Abstract. The wind tunnel campaign evaluated 10 configurations of a tractor-trailer combination using a Volvo VNL860 tractor and the 30 ft NRC trailer. The test results include balance measurements of drag force, side force, and yawing moment. The baseline tractor-trailer combination had a blockage-corrected drag coefficient of 0.457 at 0° yaw and a wind-averaged drag coefficient of 0.527. The combined removal of the side extenders, their extensions, and the roof air deflector (in Configurations 6 and 7) resulted in the largest increase in drag (6 % relative to baseline) of all of the aerodynamic packages that were evaluated. The smallest change in drag coefficient resulted from the removal of the tractor skirt extensions (aerodynamic package 4), but it should be noted that the tractor skirt extensions were only evaluated at 0 yaw and would have more of an effect at higher yaw angles. The purpose of this paper is to study the drag coefficient of the entire Tractor through wind tunnel experiments. At present, there are few tests on the resistance coefficient of Tractors, and there are also few published papers on this topic. By removing Aerodynamic packages, this helps to understand the impact of different Aerodynamic packages on the overall drag coefficient of the vehicle.

Keywords: drag coefficient, frontal reference area, aerodynamic packages, aerodynamics.

1. Introduction

Trucking industry profits are contingent on truck fuel economy, which is shaped by several factors, including their aerodynamic design [1]. The National Research Council Canada (NRC) conducted a wind tunnel campaign, from May 1 to May 2, 2019. The wind tunnel campaign evaluated 10 configurations of a tractor-trailer combination. A Volvo VNL860 tractor was used and was paired with the NRC 30ft trailer. Balance data were recorded for each configuration, including drag force, side force, and yawing moment. Smoke and yarn visualization were conducted to evaluate the flow near the hood and A-pillar. This report documents the setup of the experiment, data reduction for balance loads and the results.

2. Material and research method

Numerous situations arise where theoretical and/or computational methods fall short, either because of the problem's intricacy or the unavailability of adequate computational resources [2]. The experimental campaign was conducted in the NRC 9 m Wind Tunnel in Ottawa, Canada. A horizontal closed-circuit atmospheric facility, known as the wind tunnel, features a spacious test section measuring 9.1 meters in width, 9.1 meters in height, and 22.9 meters in length, making it ideal for conducting full-scale tests on tractor-trailer combinations. The system is driven by a 6.7 MWDC motor, capable of operating at speeds ranging from 20 to 225 rpm, with precision maintenance within ±0.1 rpm. In the empty test section, the maximum wind velocity reaches approximately 55 m/s, equivalent to 200 km/h. The area before the test section features a 6:1 contraction, moving from a circular to a filleted square cross-section. A turntable facilitates the rotation of the model around the vertical axis, enabling the simulation of crosswind effects.

Additionally, an external mechanical balance detects the various components of aerodynamic forces and moments. The turntable offers a positional resolution of 0.01 degrees. The NRC Road Traffic & Turbulence System (RT2S) encompasses two integral systems: the NRC Road Turbulence System (RTS), which was introduced in 2014, and a traffic-wake generator system, specifically introduced for this testing initiative [3].

2.1. Material

The overall setup of the Volvo VNL860 prototype tractor and NRC trailer in the Wind Tunnel as illustrated in Fig. 1. Drive-axle wheels of tractor are placed upon specially-made chock platforms that are connected to the balance. These chock platforms allow the vehicle to be rotated in yaw at angles of up to 12°. The front steering-axle wheels of the tractor and the axle wheels of the trailer are supported off-balance on horizontally unconstrained air bearings. The air bearing pads slide over floatation support surfaces mounted on the floor of the test section. The flotation support plates provide a smooth surface that is level with respect to gravity. In this configuration, drag force, side force, and yawing moment measurements are available from the six-component balance. The dimensions of the tractor, the dimensions for the trailer, and the test section layout are included in Table 1.

Fig. 1. Setup for the full-scale tractor-trailer wind tunnel experiment with the Volvo VNL860 tractor at a yaw angle of 10°

Table 1. Dimensions used for blockage corrections and normalized coefficients

Parameter	Value
Trailer Width	2591 mm
Trailer Width	4089 mm
Length, Tractor-trailer	14953 mm
Frontal Area	10.66 m^2
Tractor Mass	8747 kg
Tractor wheelbase	6628 mm
RX	740 mm

2.2. Research method

Advancements in automotive solutions are being fueled by governmental mandates and escalating consumer demands for vehicles that exhibit greater energy efficiency [4]. Reducing aerodynamic drag represents one effective strategy for enhancing energy efficiency. A diverse range of test methodologies are utilized by industry professionals, researchers, and governmental bodies to assess the aerodynamics of heavy-duty trucks [5]. Data were acquired at each specified angle for 60 seconds, following a period of dwell time to allow the wind speed, and balance to stabilize. Balance data were acquired at 20 Hz. Data were acquired at each specified angle for 60 seconds, following a period of dwell time to allow the wind speed balance to stabilize. Balance data were acquired at 20 Hz. These limits correspond to a change in drag coefficient of 0.0021, a change in side force coefficient of 0.0052, and a change in yaw moment coefficient of 0.0007. It is well-established that aerodynamic drag can be managed through two primary mechanisms: enhancing pressure recovery in the wake region and minimizing separation across the vehicle's body surfaces [5].

3. Test program and data reduction

3.1. Test program

This article presents an analysis of aerodynamic drag sensitivity for various add-on devices utilized in heavy commercial vehicles [6]. Modifying the shapes of heavy vehicles to lower aerodynamic drag can lead to reduced fuel consumption [7]. The test campaign involved force, moment taken over a range of wind speeds and yaw angles. The test program included 10 tests with a tractor-trailer combination. The test plan is shown in Table 1 and lists the various aerodynamic packages, or drag reduction technologies that were installed for a given configuration. The five aerodynamic packages (AP) that were evaluated throughout the test are shown in Fig. 2. These include the adjustable air deflector (aero package 1), the black side extender extensions (2), the main white side extenders (3), the tractor skirt extensions (4), and the sun shade (5). Photographs of the vehicle, configuration-specific test notes, and a tabulation of the drag coefficients at 0° yaw are shown in Table 2. As described in Table 2, the air deflector position was optimized for the space width between the tractor and trailer. The bottom mounting hole on the air deflector arm and the third (middle) hole on the air deflector mounting bracket were used throughout the test.

Table 2. Test plan and description of configurations. The blockage-corrected wind speeds are shown in the last column

Configuration	Client description	Aero packages (AP) on vehicle	Turntable yaw angle [deg]	Wind speed [km/h]
1	Design vehicle with pressure measurements	All	0	[80, 85, 90, 95, 120]
1	Design vehicle with pressure measurements	All	[0, 1, 2, 5, 10, 12]	95
2	Design vehicle (pressure taps removed)	All	0	[80, 85, 90, 95, 120]
2	Design vehicle (pressure taps removed)	All	[0, 1, 2, 5, 10, 12]	95
3	Remove AP 2 (Install AP 1, 3, 4, 5)	1, 3, 4, 5	0	95
4	Remove AP1+2 (Install AP 3, 4, 5)	3, 4, 5	0	95
5a	Remove AP1 (Install AP 2, 3, 4, 5)	2, 3, 4, 5	0	95
5b	Remove AP1 (Install AP 2, 3, 4, 5)	2, 3, 4, 5	0	95
6	Remove AP 1+2+3 (Install AP 4, 5)	4, 5	0	95
7	Remove AP 1+2+3+4 (Install AP 5)	5	0	95
8	Remove AP4 (Install AP 1, 2, 3, 5)	1, 2, 3, 5	0	95
9	Remove AP5 (Install AP 1, 2, 3, 4)	1, 2, 3,4	0	95
10	Baseline repeat	All	0	95
10	Flow visualization	All	0	30

Fig. 2. Aerodynamic packages that were removed or installed during the test

3.2. Balance coefficients

The resistance exerted by air on a moving vehicle is termed aerodynamic drag force [8]. These measured data are transformed into the body axis and are provided as coefficients. The yaw direction (ψ) is positive clockwise when viewed from above. The yaw angle is corrected for wall effects using standard wall corrections. Hence, to diminish the drag force, alterations can solely be made to the Coefficient of Drag (Cd) and the frontal area (A), as both air density and vehicle velocity are predetermined by atmospheric conditions and regulatory speed limits for trucks. To decrease aerodynamic drag, the key lies in reducing the product of Cd × A [9].

4. Results

Test results include tabulated force and moment coefficient data, which are provided separately in comma-separated-value format. Force and moment coefficients are provided with and without blockage corrections in the comma-separated-value files, but only blockage-corrected results are shown in the report. The test results also include, in electronic format separate from the report, photographs and recorded video of flow visualization in the test section. The results shown below highlight the moment coefficients and force of the baseline vehicle and the configurations with the drag-reduction technologies removed.

4.1. Baseline vehicle combinations

Force and moment coefficients for the original vehicle state are compared with (Configuration 1) and without (Configuration 2) pressure taps in Fig. 3. Fig. 3(a) plots the speed sweep results and Fig. 3(b) plots the yaw sweep conducted in both configurations. The wind speed in Fig. 3(a) has been corrected for blockage effects and the yaw angle shown in Fig. 3(b) has been corrected for wall effects.

The presence of the pressure taps in Configuration 1 did not have a significant impact on the drag, side, and yawing moment coefficients. It should be noted that two yaw sweeps (Runs 28 and 29) were conducted for Configuration 1. Only the balance data from Run 29 are shown in Fig. 3(b). However, the pressure data between these two repeat runs are compared below. The wind-averaged drag coefficient for Configuration 1 (Run 29) was 0.527 and the wind-averaged drag coefficient for Configuration 2 (Run 32) was 0.527, based on a vehicle ground speed of 95 km/h. Additionally, the difference in the drag coefficient at 0° between these two configurations corresponded to a change in drag coefficient of 0.0024 (% difference of 0.5 %).

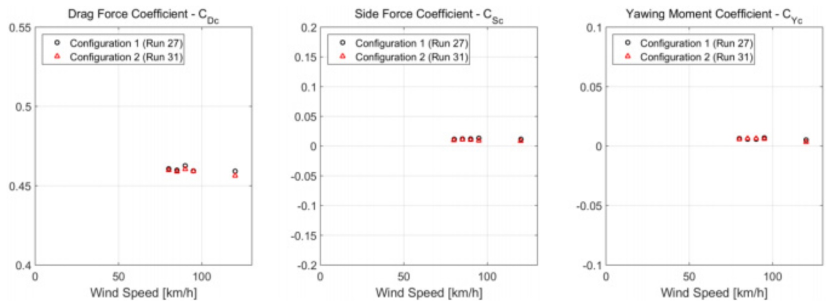

a) Speed sweep

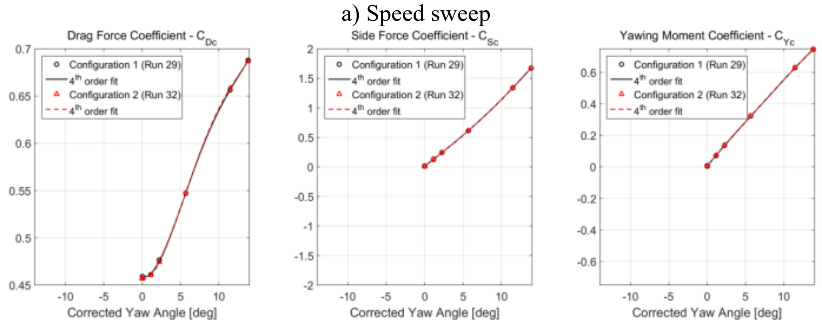

b) Yaw sweep

Fig. 3. Force and moment coefficients for the baseline vehicle (Configuration 1: with pressure measurements. Configuration 2: without pressure measurements)

4.2. Effect of drag reduction technologies

Throughout the test campaign, five aerodynamic packages were removed from the vehicle. These devices were shown earlier in Fig. 2. The drag coefficient at 0° and at 95 km/h for each configuration is shown in Fig. 4(a). For the yaw sweeps conducted for Configurations 1 and 2, the average of the drag coefficients for the 0° data points in the yaw sweep was used in the comparison. The change in drag (ΔCD) associated wit a particular configuration was calculated by comparing the drag coefficient to a baseline reference case. Configurations 1 to 5a use Configuration 2 as a baseline, whereas Configurations 5b to 9 use Configuration 10 as a baseline. This was due to the variability associated with the re-installation of aero package 2 in Configuration 5a. The challenges associated with the positioning and repeatability of the installation of aerodynamic package 2 are documented in Table 2. Aerodynamic package 2 was adjusted in Configuration 5b and was maintained for the duration of the test.

An interesting observation was an interaction between the air deflector (aero package 1) and the side extender extensions (aero package 2). The removal of only aero package 2 in Configuration 3 resulted in a small increase in drag. When aero packages 1 and 2 were removed in Configuration 4, a larger increase in drag was observed. When only aero package 1 was removed in Configuration 5a, the magnitude of the drop was much larger than the magnitude of the increase seen for Configuration 3. This seems to indicate that the presence of one component alone (either the side extender extensions or the air deflector) has a dominant effect at controlling the flow in the gap.

The removal of aero packages 1, 2, and 3 (Configurations 6 and 7) resulted in the largest increase in drag coefficient (increase of 6 % compared to Configuration 10). The removal of the tractor skirt extensions in Configurations 7 and 8 did not have a significant impact on the drag coefficient obtained at 0° yaw, although it is expected that they would have a more significant influence when the vehicle is yawed. The removal of the sun shade in Configuration 9 resulted in a drop in drag coefficient of 0.0024, indicating that the sun shade has been optimized to have only a minor influence on drag.

ISSN PRINT 2345-0533, ISSN ONLINE 2538-8479

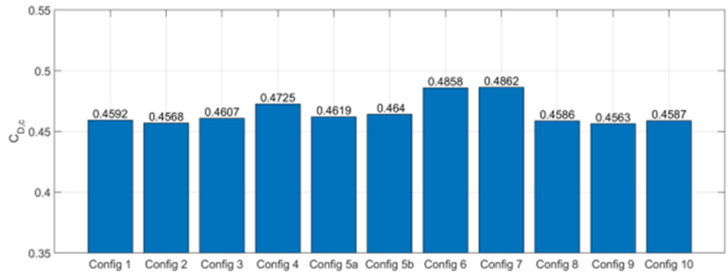

a) CD, c

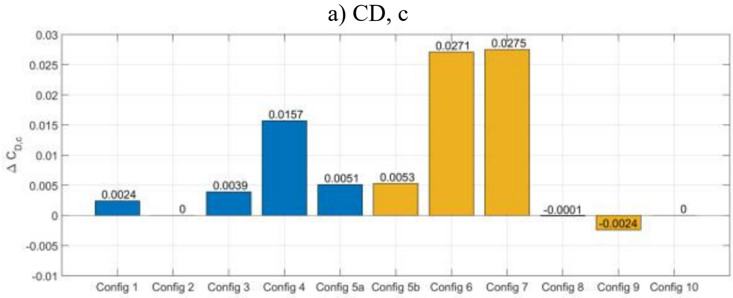

b) ΔCD, c, relative to baseline. Configurations 1 to 5auseConfiguration 2 as a baseline and Configurations 5b to 9 use Configuration 10 as a baseline

Fig. 4. Effect of drag reduction technologies on the blockage-corrected drag coefficient at 0° yaw and at 95 km/h

Depending on the vehicle configuration and vehicle weight, the fuel consumption used for aerodynamic drag and the fuel consumption used for rolling resistance are approximately equal at 100 km/h for a vehicle weighing 97,000 lb. A rough approximation of the effect of an aerodynamic drag reduction on overall fuel consumption is that the overall fuel consumption would be reduced by half of the magnitude of the reduction in aerodynamic drag. A 6 % change in aerodynamic drag coefficient roughly corresponds to a 3 % change in overall fuel consumption, depending on vehicle speed, weight, and rolling resistance. Another method of determining the potential fuel savings from drag measurements is used by the US Environmental Protection Agency (EPA) Smart Way program. The method estimates fuel savings based on the percent change in wind-averaged drag and a conversion factor. For a vehicle travelling at 65 mph, the percent change in wind-averaged drag is divided by a factor of 1.85 to estimate the percentage of fuel savings associated with a particular technology.

5. Conclusions

The wind tunnel campaign evaluated 10 configurations of a tractor-trailer combination using a Volvo VNL860 that was paired with the NRC 30 ft trailer. The report summarized the experimental setup, and presented the balance. The appendices contain a description of the configurations, dimensions, and test section layout. The baseline tractor-trailer combination had a blockage-corrected drag coefficient of 0.457 at 0°yaw and a wind-averaged drag coefficient of 0.527. The combined removal of the side extenders, their extensions, and the roof air deflector (in Configurations 6 and 7) resulted in the largest increase in drag (6 % relative to baseline) of all of the aerodynamic packages that were evaluated. The smallest change in drag coefficient resulted from the removal of the tractor skirt extensions (aerodynamic package 4), but it should be noted that the tractor skirt extensions were only evaluated at 0° yaw and would have more of an effect at higher yaw angles. Aerodynamic interactions were observed between the air deflector (aerodynamic package 1) and the side extender extensions (aerodynamic package 2) where the flow in the gap appeared to be controlled predominantly by the installation of a single component for the gap width that was evaluated. The side extender extensions (aerodynamic package 2) were difficult to reinstall in the exact same position, due to the presence of thick double-sided tape at the mounting location and the flexibility of the plastic material. As a result, the first half of the test used Configuration 2 as a baseline and the second half of the test used Configuration 10 as a baseline. This article fully demonstrates the relevant data of the Tractor wind tunnel test process. It can fill the gap in related research. This paper introduces multiple schemes, which can clearly understand the impact of each scheme on the overall wind resistance of the vehicle. Due to the limited number of wind tunnels for vehicles and trucks, and the limited publication of related papers, this article can effectively fill the relevant gaps.

Acknowledgements

The authors have not disclosed any funding.

Data availability

The datasets generated during and/or analyzed during the current study are available from the corresponding author on reasonable request.

Conflict of interest

The authors declare that they have no conflict of interest.

References

[1] I. V. Gritsuk, O. Batrachenko, L. Tarandushka, V. Mitienkova, O. Bazhinov, and T. Bazhynova, “Rationale for new ways to reduce the aerodynamic resistance of road trains,” *Automotive Technical Papers*, Sep. 2022, https://doi.org/10.4271/2022-01-5080

[2] L. Cattafesta, C. Bahr, and J. Mathew, “Fundamentals of wind-tunnel design,” in *Encyclopedia of Aerospace Engineering*, Wiley, 2010, pp. 1–10, https://doi.org/10.1002/9780470686652.eae532

[3] B. Mcauliffe, H. Barber, and F. Ghorbanishohrat, “The influence of traffic wakes on the aerodynamic performance of heavy duty vehicles,” *SAE International Journal of Advances and Current Practices in Mobility*, Vol. 5, No. 6, pp. 2193–2214, Apr. 2023, https://doi.org/10.4271/2023-01-0919

[4] J. Törnell, S. Sebben, and P. Elofsson, “Influence of yaw and lateral offset on the aerodynamics of a two-truck platoon,” *SAE International Journal of Commercial Vehicles*, Vol. 16, No. 2, pp. 153–164, Oct. 2022, https://doi.org/10.4271/02-16-02-0010

[5] J. W. Hawkins, H. Kowalczyk, and D. Johnson, “Computational fluid dynamics model creation and simulation for class 8 tractor-trailers,” *Automotive Technical Papers*, Aug. 2023, https://doi.org/10.4271/2023-01-5051

[6] M. Velshankar, S. Senthilkumar, and B. T. Kannan, “Aerodynamic drag reduction of an intercity bus through surface modifications – a numerical simulation,” in *International Conference on Advances in Design, Materials, Manufacturing and Surface Engineering for Mobility*, Oct. 2019, https://doi.org/10.4271/2019-28-0045

[7] F. Anwar, R. A. Gulavani, S. Chalipat, and S. Jadhav, “Aero drag improvement study on large commercial vehicles using CFD lead approach,” in *Symposium on International Automotive Technology*, Sep. 2021, https://doi.org/10.4271/2021-26-0424

[8] R. Mccallen et al., “Progress in reducing aerodynamic drag for higher efficiency of heavy duty trucks (Class 7-8),” in *Government/Industry Meeting*, Apr. 1999, https://doi.org/10.4271/1999-01-2238

[9] F. L. Zarpelon, L. Balcewicz, L. Formolo, and R. Guarda, “Aerodynamic analysis of a concept truck and trailer for grain transportation,” in *12th SAE BRASIL Colloquium on Suspensions and Road Implements and Engineering Exhibition*, Jul. 2023, https://doi.org/10.4271/2023-36-0353